Measurement of the neutrino magnetic moment at the NOvA experiment

Technical note

Robert Kralik[1]

[1]University of Sussex, Brighton, UK

February 9, 2024

Abstract

This is the abstract

Contents

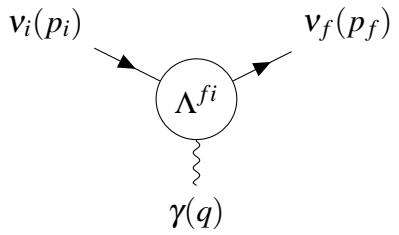

Figure 1: Effective coupling of neutrinos with one photon electromagnetic field.

1 Introduction

(TO DO: *Describe the main motivations for the analysis. Briefly mention that there was a previous study by Biao, what were the results there and what limitations (or maybe talk about this in the Experimental overview?)*)

2 Theoretical overview

(TO DO: *Re-read the three main theory papers and double check the theoretical overview*)

In the Standard Model (SM), neutrinos are massless and electrically neutral particles. However, even in the SM neutrinos can have electromagnetic interaction through loop diagrams involving the charged leptons and the W boson. These interactions are described by the neutrino charge radius, described in section 2.2 [1].

To include neutrino masses required by neutrino oscillations, we must go Beyond the Standard Model (BSM), where neutrinos can acquire other electromagnetic properties [2]. In the most general case, considering interactions with a single photon as shown on Fig.1, neutrino electromagnetic interactions can be described by an *effective* interaction Hamiltonian [2]

$$\mathscr{H}_{em}^{(\nu)}(x) = \sum_{k,j=1}^{N} \overline{\nu}_k(x) \Lambda_\mu^{kj} \nu_j(x) A^\mu(x). \tag{1}$$

Here $\nu_k(x), k \in \{1,...,N\}$ are neutrino fields in the mass basis with N neutrino mass states. Λ_μ^{kj} is a general vertex function and $A^\mu(x)$ is the electromagnetic field.

The vertex function $\Lambda_\mu^{fi}(q)$ is generally a matrix and in the most general case can be written in terms of linearly independent products of Dirac matrices (γ) and only depends on the square of the four momentum of the photon $\left(q = p_f - p_i\right)$:

$$\begin{aligned}\Lambda_\mu^{fi}(q) =& \mathbb{F}_1^{fi}\left(q^2\right) q_\mu + \mathbb{F}_2^{fi}\left(q^2\right) q_\mu \gamma_5 + \mathbb{F}_3^{fi}\left(q^2\right) \gamma_\mu + \mathbb{F}_4^{fi}\left(q^2\right) \gamma_\mu \gamma_5 + \\ & \mathbb{F}_5^{fi}\left(q^2\right) \sigma_{\mu\nu} q^\nu + \mathbb{F}_6^{fi}\left(q^2\right) \varepsilon_{\mu\nu\rho\gamma} q^\nu \sigma^{\rho\gamma},\end{aligned} \tag{2}$$

where $\mathbb{F}_i^{fi}\left(q^2\right)$ are six Lorentz invariant form factors [2].

Applying conditions of hermiticity $\left(\mathscr{H}_{em}^{(\nu)\dagger} = \mathscr{H}_{em}^{(\nu)}\right)$ and of the gauge invariance of the electromagnetic field, we can rewrite the vertex function as

$$\Lambda_{\mu}^{fi}(q) = \left(\gamma_{\mu} - q_{\mu}\not{q}/q^2\right)\left[\mathbb{F}_{Q}^{fi}\left(q^2\right) + \mathbb{F}_{A}^{fi}\left(q^2\right)q^2\gamma_5\right] - i\sigma_{\mu\nu}q^{\nu}\left[\mathbb{F}_{M}^{fi}\left(q^2\right) + i\mathbb{F}_{E}^{fi}\left(q^2\right)\gamma_5\right], \quad (3)$$

where $\mathbb{F}_{Q}^{fi}, \mathbb{F}_{M}^{fi}, \mathbb{F}_{E}^{fi}$ and $\mathbb{F}_{A}^{fi}$ are hermitian matrices representing the charge, dipole magnetic, dipole electric and anapole neutrino form factors. In coupling with a real photon $\left(q^2 = 0\right)$ these become the neutrino charge and magnetic, electric and anapole moments. The neutrino charge radius corresponds to the second term in the expansion of the charge form factor [2].

We can simplify the above expression as [1]

$$\Lambda_{\mu}^{fi}(q) = \gamma_{\mu}\left(Q_{\nu_{fi}} + \frac{q^2}{6}\langle r^2\rangle_{\nu_{fi}}\right) - i\sigma_{\mu\nu}q^{\nu}\mu_{\nu_{fi}}, \quad (4)$$

where $Q_{\nu_{fi}}$, $\langle r^2\rangle_{\nu_{fi}}$, and $\mu_{\nu_{fi}}$ are the neutrino charge, effective charge radius (also containing anapole moment), and an effective magnetic moment (also containing electric moment) respectively. This is possible thanks to the proportional effect of the neutrino charge radius and the anapole moment, or the neutrino magnetic and electric moment respectively [2]. These quantities (charge, charge radius and magnetic moment) are the three neutrino electromagnetic properties measured in experiments.

2.1 Neutrino electric and magnetic dipole moments

The size and effect of the neutrino electromagnetic properties depends on the specific theory beyond the standard model.

Evaluating the one loop diagrams in the minimal extension of the standard model with three right handed Dirac neutrinos gives us the first approximation of the electric and magnetic moments:

$$\left.\begin{matrix}\mu_{kj}^{D} \\ i\varepsilon_{kj}^{D}\end{matrix}\right\} \simeq \frac{3eG_F}{16\sqrt{2}\pi^2}\left(m_k \pm m_j\right)\left(\delta_{kj} - \frac{1}{2}\sum_{l=e,\mu,\tau}U_{lk}^{\star}U_{lj}\frac{m_l^2}{m_W^2}\right), \quad (5)$$

where m_k, m_j are the neutrino masses and m_l are the masses of charged leptons which appear in the loop diagrams [2]. e is the electron charge, G_F is the Fermi coupling constant, and U is the PMNS neutrino oscillation matrix. Higher order electromagnetic corrections were neglected, but those can also have a significant contribution, depending on the theory.

It can be seen that there dirac neutrinos have no diagonal electric moments $\left(\varepsilon_{kk}^{D} = 0\right)$ and their diagonal magnetic moments are approximately

$$\mu_{kk}^{D} \simeq \frac{3eG_F m_k}{8\sqrt{2}\pi^2} \simeq 3.2\times10^{-19}\left(\frac{m_k}{\mathrm{eV}}\right)\mu_B, \quad (6)$$

where μ_B is the Bohr magneton [2].

The transition magnetic moments are suppressed with respect to the largest of the diagonal magnetic moments by at least a factor of 10^{-4} due to the m_W^2 in the denominator. The transition

electric moments are even smaller due to the mass difference in Eq.5. Therefore an experimental observation of a magnetic moment larger than in Eq.6 would indicate physics beyond the minimally extended standard model [2, 3].

Majorana neutrinos in a minimal extension can be obtained by either adding a $\mathrm{SU}(2)_L$ Higgs triplet, or right handed neutrinos together with a $\mathrm{SU}(2)_L$ Higgs singlet [2]. If we neglect the Feynman diagrams which depend on the model of the scalar sector, the magnetic and electric dipole moments are

$$\mu_{kj}^M \simeq -\frac{3ieG_F}{16\sqrt{2}\pi^2}\left(m_k + m_j\right)\sum_{l=e,\mu,\tau}\mathrm{Im}\left[U_{lk}^\star U_{lj}\right]\frac{m_l^2}{m_W^2}, \tag{7}$$

$$\varepsilon_{kj}^M \simeq \frac{3ieG_F}{16\sqrt{2}\pi^2}\left(m_k - m_j\right)\sum_{l=e,\mu,\tau}\mathrm{Re}\left[U_{lk}^\star U_{lj}\right]\frac{m_l^2}{m_W^2}. \tag{8}$$

These are difficult to compare to the Dirac case, due to possible presence of Majorana phases in the PMNS matrices, but it is clear that they have the same order of magnitude as Dirac transition dipole moments. However, the neglected model dependent contributions can enhance the transition dipole moments [2].

It is possible [3] to obtain a "natural" upper limits on the size of neutrino magnetic moment by calculating its contribution to the neutrino mass by standard model radiative corrections. For Dirac neutrinos, the radiative correction induced by neutrino magnetic moment, generated at an energy scale Λ, to the neutrino mass is generically

$$m_\nu^D \sim \frac{\mu_\nu^D}{3\times 10^{-15}\mu_B}\left[\Lambda\,(\mathrm{TeV})\right]^2\mathrm{eV}. \tag{9}$$

So for $\Lambda \simeq 1\mathrm{TeV}$ (TO DO: *figure out what exactly does this energy scale actually relate to and explain it here?*) and $m_\nu \lesssim 0.3\mathrm{eV}$ the limit becomes $\mu_\nu^D \lesssim 10^{-15}\mu_B$. This applies only if the new physics is well above the electroweak scale ($\Lambda_{EW} \sim 100\mathrm{GeV}$). It is possible to get Dirac neutrino magnetic moment higher than this limit, for example in frameworks of minimal super-symmetric standard model, by adding more Higgs doublets, or by considering large extra dimensions [2].

A similar limit for Majorana neutrino magnetic moment would be less stringent due to the antisymmetry of the Majorana neutrino magnetic moment form factors. Considering $m_\nu \lesssim 0.3\mathrm{eV}$, the limit can be expressed as

$$\mu_{\tau\mu}, \mu_{\tau e} \lesssim 10^{-9}\left[\Lambda\,(\mathrm{TeV})\right]^{-2} \tag{10}$$

$$\mu_{\mu e} \lesssim 3\times 10^{-7}\left[\Lambda\,(\mathrm{TeV})\right]^{-2} \tag{11}$$

which is shown in the flavour basis [3]. This expression relates to the framework used previously as

$$\mu_{ij} = \sum_{\alpha\beta}\mu_{\alpha\beta}U_{\alpha i}^\star U_{\beta j}, \quad \alpha,\beta \in \{e,\mu,\tau\}. \tag{12}$$

These considerations imply, that if a magnetic moment $\mu \gtrsim 10^{-15}\mu_B$ would be measured, it is more plausible that neutrinos are Majorana fermions and that the scale of lepton violation would be well below the conventional see-saw scale [3] (TO DO: *double check this claim*).

2.1.1 Effective neutrino magnetic moment

Since experiments detect neutrino flavour states, not the mass states, what we measure in experiments is an effective "flavour" magnetic moment μ_{eff}. μ_{eff} is influenced by mixing of the neutrino magnetic moments (and electric moments) expressed in the mass basis (as described above) and neutrino oscillations. In the ultra-relativistic limit, the (anti)neutrino effective magnetic moment is

$$\mu^2_{\nu_l}(L,E_\nu) = \sum_j \left| \sum_k U^\star_{lk} e^{\mp i\Delta m^2_{kj} L/2E_\nu} \left(\mu_{jk} - i\varepsilon_{jk}\right) \right|^2 , \tag{13}$$

where L is the distance the neutrino travelled, E_ν is the neutrino energy and δm^2 is the neutrino mass squared difference [2]. The minus sign in the exponent is for neutrinos and the plus sign for antineutrinos, therefore the only difference is in the phase induced by neutrino oscillations.

For experiments with baselines short enough that neutrino oscillations would not have time to develop $\left(\Delta m^2 L/2E_\nu \ll\sim 1\right)$, such as the NOvA Near Detector, the effective magnetic moment can be expressed as

$$\mu^2_{\nu_l} = \mu^2_{\bar{\nu}_l} \simeq \sum_j \left| \sum_k U^\star_{lk} \left(\mu_{jk} - i\varepsilon_{jk}\right) \right|^2 = \left[U\left(\mu^2 + \varepsilon^2\right) U^\dagger + 2\,\mathrm{Im}\left(U\mu\varepsilon U^\dagger\right) \right]_{ll'} , \tag{14}$$

which is independent of the neutrino energy and of the source to detector distance.

It is important to mention, that since the effective magnetic moment depends on the flavour of the studied neutrino, it is different (but related) for neutrino experiment studying neutrinos from different sources. Additionally some experiments, namely solar neutrino experiments, need to include matter effects on the neutrino oscillations. Therefore the reports on the value (or upper limit) of the effective neutrino magnetic moment are not directly comparable between different types of neutrino experiments. Theorists publish papers trying to extrapolate the measured effective magnetic moments to each neutrino flavour, but necessarily apply assumptions that might not hold in all BSM theories.

2.2 Other neutrino electromagnetic properties

(TO DO: *This section is not finished, most of this text is just copied from some theory papers for now*)

Neutrino electric charge is heavily constraint by the measurements on the neutrality of matter (since generally neutrinos having an electric charge would also mean that neutrons have charge which would affect all heavier nuclei). It is also constrained by the SN1987A, since neutrino having an effective charge would lengthen its path through the extragalactic magnetic fields and would arrive on earth later. It can also be obtained from nu-on-e scatter from the relationship between neutrino millicharge and magnetic moment. [nuElmagInt2015.pdf - sec. VIIA]

The neutrino charge radius is determined by the second term in the expansion of the neutrino charge form factor and can be interpreted using the Fourier transform of a spherically symmetric

charge distribution. It can also be negative since the charge density is not a positively defined quantity. In the SM the charge radius has the form of (possible other definitions exist)

$$\langle r^2_{\nu_l}\rangle_{\mathsf{SM}} = \frac{G_{\mathsf{F}}}{4\sqrt{2}\pi^2}\left[3 - 2\log\left(\frac{m_l^2}{m_W^2}\right)\right]. \tag{15}$$

This corresponds to $\langle r^2_{\nu_\mu}\langle_{\mathsf{SM}} = 2.4\times10^{-33}$ cm^2 and similar scale for other neutrino flavours. [nuElmagInt2015.pdf - sec. VIIB]

[nuElmagInt2015.pdf - sec. VIIB] The effect of the neutrino charge radius on the neutrino-on-electron scattering cross section is through the following shift of the vector coupling constant (Grau and Grifols, 1986; Degrassi, Sirlin, and VMarciano, 1989; Vogel and Engel, 1989; Hagiwara et al., 1994):

$$g_V^{\nu_l} \to g_V^{\nu_l} + \frac{2}{3}m_W^2\langle r^2_{\nu_l}\rangle \sin^2\theta_W \tag{16}$$

[nuElmagInt2015.pdf - sec. VIIB] The current experimental limits for muon neutrinos are from (TO DO: *check the current exp. limits*) Hirsch, Nardi, and Restrepo (2003) who obtained the following 90% C.L. bounds on $\langle r^2_{\nu_\mu}\rangle$ from a reanalysis of CHARM-II (Vilain et al., 1995) and CCFR (McFarland et al.,1998) data:

$$-0.52\times10^{-32} < \langle r^2_{\nu_\mu}\rangle < 0.68\times10^{-32}\ \text{cm}^2 \tag{17}$$

In the Standard Model, the neutrino anapole moment is somehow coupled with the neutrino charge radii and is functionally identical. the phenomenology of neutrino anapole moments is similar to that of neutrino charge radii. Hence, the limits on the neutrino charge radii discussed in Sec. VII.B also apply to the neutrino anapole moments multiplied by 6. in the standard model the neutrino charge radius and the anapole moment are not defined separately and one can interpret arbitrarily the charge form factor as a charge radius or as an anapole moment. Therefore, the standard model values for the neutrino charge radii in Eqs. (7.35)–(7.38) can be interpreted also as values of the corresponding neutrino anapole moments. [nuElmagInt2015.pdf - sec. VIIC]

It is possible to consider the toroidal dipole moment as a characteristic of the neutrino which is more convenient and transparent than the anapole moment for the description of T-invariant interactions with nonconservation of the P and C symmetries. the toroidal and anapole moments coincide in the static limit when the masses of the initial and final neutrino states are equal to each other. The toroidal (anapole) interactions of a Majorana as well as a Dirac neutrino are expected to contribute to the total cross section of neutrino elastic scattering off electrons, quarks, and nuclei. Because of the fact that the toroidal (anapole) interactions contribute to the helicity preserving part of the scattering of neutrinos on electrons, quarks, and nuclei, its contributions to cross sections are similar to those of the neutrino charge radius. In principle, these contributions can be probed and information about toroidal moments can be extracted in low-energy scattering experiments in the future. Different effects of the neutrino toroidal moment are discussed by Ginzburg and Tsytovich (1985), Bukina, Dubovik, and Kuznetsov (1998a, 1998b), and Dubovik and Kuznetsov (1998). In particular, it has been shown that the neutrino toroidal electromagnetic interactions can produce Cherenkov radiation of neutrinos propagating in a medium. [nuElmagInt2015.pdf - sec. VIIC]

2.3 Measuring neutrino magnetic moment

The most sensitive method to measure neutrino magnetic moment is the low energy elastic scattering of (anti)neutrinos on electrons [2]. The diagram for this interaction is shown on Fig.2 showing the two observables, the recoil electron's kinetic energy ($T_e = E_{e\prime} - m_e$) and the recoil angle with respect to the incoming neutrino beam (θ).

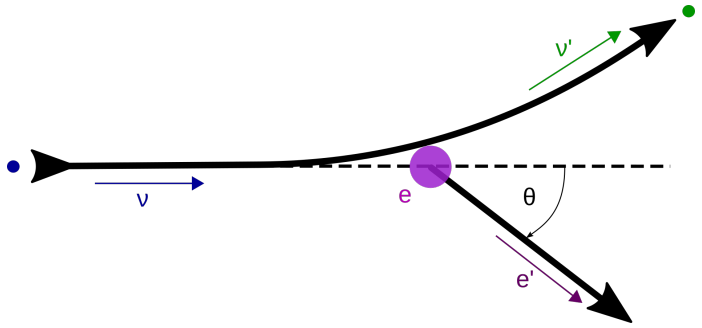

Figure 2: Neutrino-on-electron elastic scattering diagram

From simple $2 \to 2$ kinematics we can calculate

$$(P_\nu - P_{e'})^2 = (P_{\nu'} - P_e)^2, \tag{18}$$

$$m_\nu^2 + m_e^2 - 2E_\nu E_{e'} + 2E_\nu p_{e'} \cos\theta = m_\nu^2 + m_e^2 - 2E_{\nu'} m_e. \tag{19}$$

Using the energy conservation

$$E_\nu + m_e = E_{\nu'} + E_{e'} = E_{\nu'} + T_e + m_e \Rightarrow E_{\nu'} = E_\nu - T_e \tag{20}$$

we get

$$E_\nu p_{e'} \cos\theta = E_\nu E_{e'} - E_{\nu'} m_e = E_\nu (T_e + m_e) - (E_\nu - T_e) m_e = T_e (E_\nu + m_e), \tag{21}$$

$$\cos\theta = \frac{E_\nu + m_e}{E_\nu} \sqrt{\frac{T_e^2}{E_{e'}^2 - m_e^2}} = \frac{E_\nu + m_e}{E_\nu} \sqrt{\frac{T_e^2}{T_e^2 + 2T_e m_e}}. \tag{22}$$

And finally we get

$$\cos\theta = \frac{E_\nu + m_e}{E_\nu} \sqrt{\frac{T_e}{T_e + 2m_e}}. \tag{23}$$

Electron's kinetic energy is kinematically constrained by the energy conservation as

$$T_e \leq \frac{2E_\nu^2}{2E_\nu + m_e}. \tag{24}$$

Considering $E_\nu \sim$ GeV, we can approximate $\frac{m_e^2}{E_\nu^2} \to 0$ and from Fig.3 we can see that we can approximate all recoil angles to be very small, therefore $\theta^2 \cong \left(1 - \cos^2\theta\right)$. Using Eq.23 we get

$$T_e \theta^2 \cong T_e \left(1 - \left(\frac{E_\nu + m_e}{E_\nu}\right)^2 \frac{T_e}{T_e + 2m_e}\right) = T_e \left(1 - \left(1 + \frac{2m_e}{E_\nu}\right) \frac{T_e}{T_e + 2m_e}\right), \tag{25}$$

therefore

$$T_e\theta^2 \cong \frac{2m_eT_e}{T_e+2m_e}\left(1-\frac{T_e}{E_\nu}\right) = 2m_e\left(\frac{1}{1+\frac{2m_e}{T_e}}\right)\left(1-\frac{T_e}{E_\nu}\right), \tag{26}$$

and finally

$$T_e\theta^2 \cong 2m_e\left(1-\frac{T_e}{E_\nu}\right) < 2m_e. \tag{27}$$

This is a strong limit that clearly distinguishes the neutrino-on-electron elastic scattering events from other similar interaction involving single electron (mainly the ν_e Charged Current interaction).

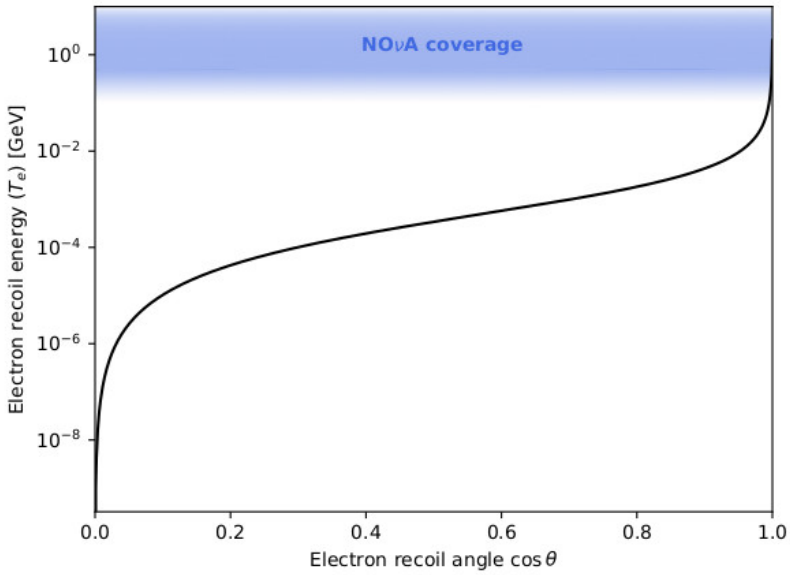

Figure 3: Relation between the recoil electron's kinetic energy and angle for neutrino-on-electron elastic scattering. The coverage of the NOvA detectors for measuring the electron recoil energy is shown in blue. Only very forwards electron's are recorded in NOvA.

2.3.1 Neutrino magnetic moment cross section

In the ultrarelativistic limit, the neutrino magnetic moment changes the neutrino helicity, turning active neutrinos into sterile (TO DO: *this is a very strong statement and it probably need a bit more backing up*). Since the SM weak interaction conserves helicity we can simply add the two contribution to the neutrino-on-electron cross section incoherently [2]:

$$\frac{d\sigma_{\nu_l e^-}}{dT_e} = \left(\frac{d\sigma_{\nu_l e^-}}{dT_e}\right)_{\text{SM}} + \left(\frac{d\sigma_{\nu_l e^-}}{dT_e}\right)_{\text{MAG}}. \tag{28}$$

The standard model contribution can be expressed as [2]:

$$\left(\frac{d\sigma_{\nu_l e^-}}{dT_e}\right)_{\mathrm{SM}} = \frac{G_F^2 m_e}{2\pi}\left\{\left(g_V^{\nu_l}+g_A^{\nu_l}\right)^2+\left(g_V^{\nu_l}-g_A^{\nu_l}\right)^2\left(1-\frac{T_e}{E_\nu}\right)^2+\left(\left(g_A^{\nu_l}\right)^2-\left(g_V^{\nu_l}\right)^2\right)\frac{m_e T_e}{E_\nu^2}\right\}, \tag{29}$$

where the coupling constants g_V and g_A are different for different neutrino flavours and for antineutrinos. Their values are:

$$g_V^{\nu_e} = 2\sin^2\theta_W + 1/2, \qquad g_A^{\nu_e} = 1/2, \tag{30}$$

$$g_V^{\nu_{\mu,\tau}} = 2\sin^2\theta_W - 1/2, \qquad g_A^{\nu_{\mu,\tau}} = -1/2. \tag{31}$$

For antineutrinos $g_A \to -g_A$.

The neutrino magnetic moment contribution is (TO DO: *include derivation from [4]*) [2]:

$$\left(\frac{d\sigma_{\nu_l e^-}}{dT_e}\right)_{\mathrm{MAG}} = \frac{\pi\alpha^2}{m_e^2}\left(\frac{1}{T_e}-\frac{1}{E_\nu}\right)\left(\frac{\mu_{\nu_l}}{\mu_B}\right)^2, \tag{32}$$

where α is the fine structure constant.

Comparison of the Standard Model and the neutrino magnetic moment cross sections is shown on Fig.4. Whereas the SM cross section is flat with $T_e \to 0$, the νMM cross section keeps increasing to infinity. However, this reach is limited by the experimental capabilities of detecting such low energetic neutrinos. Possible NOvA coverage is shown in a shaded blue and it is uncertain we could actually reach as low as 100 MeV.

(TO DO: *Reference the colours on the figures to the origins of the values (LSND and Biao)*)

As can be seen on Fig.4 and Fig.5, the magnetic moment contribution exceeds the standard model contribution for low enough T_e. This can be approximated as [2]:

$$T_e \lesssim \frac{\pi^2\alpha^2}{G_F^2 m_e^3}\left(\frac{\mu_\nu}{\mu_B}\right)^2 \simeq 2.9\times 10^{19}\left(\frac{\mu_\nu}{\mu_B}\right)^2\,[\mathrm{MeV}], \tag{33}$$

which does not depend on the neutrino energy and makes experiments sensitive to lower energetic electrons more sensitive to the neutrino magnetic moment. This is especially true for the recent dark matter experiments which put stringent limits on the solar neutrino effective magnetic moment, as described in the following section.

2.3.2 Neutrino on nucleus scattering

(TO DO: *not sure this is actually needed, but there are a few papers on this topic so might be worth mentioning it here. Although i don't think NOvA would be able to use this ever*)

2.3.3 Cosmological effects

(TO DO: *This is an unfinished section and most of this text is just copied from some references. I find it interesting and would like to include some information on this, but haven't had time yet*)

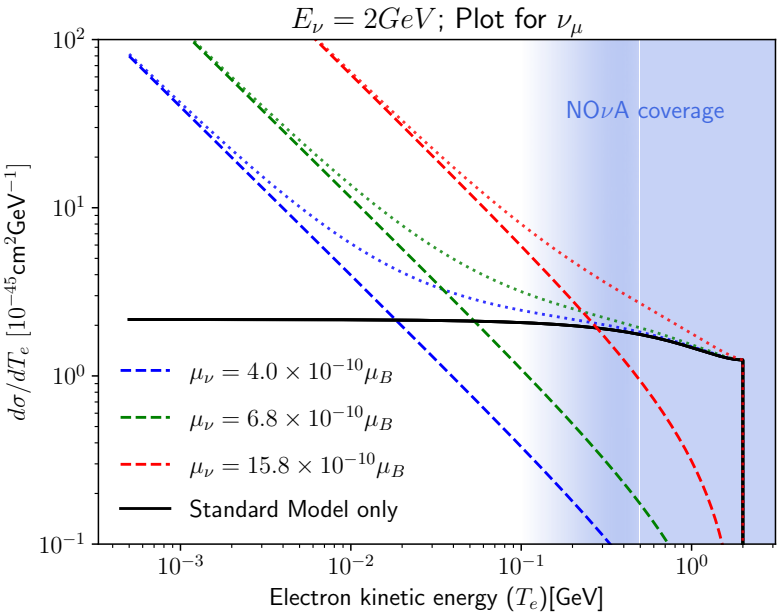

Figure 4: Comparison of the neutrino magnetic moment (coloured) and Standard Model (black) cross sections for the neutrino-on-electron elastic scattering. Different colours depict different values of the neutrino magnetic moment. Dashed lines are the individual cross sections and dotted lines are the added total cross section with the standard model contribution. NOvA coverage of electron recoil energies is shown in shaded blue.

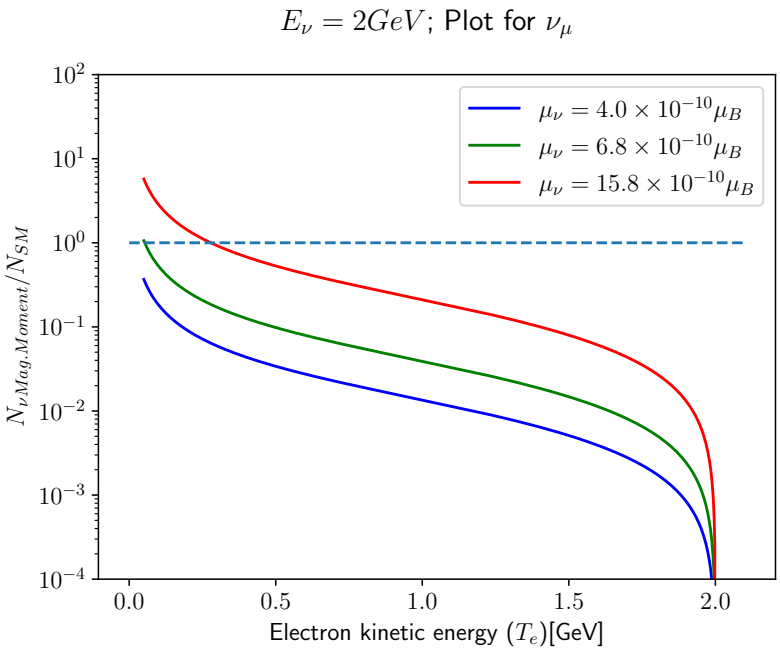

Figure 5: Ratio of the netrino magnetic moment cross section to the standard model cross section for the neutrino-on-electron elastic scattering. Different colours depict different effective muon neutrino magnetic moment values.

[NuMMBasicsAndAstro_2022.pdf] One of the most important astrophysical consequences of neutrino non-zero effective magnetic moments is the neutrino helicity change $\nu_l \rightarrow \nu_R$ with the appearance of nearly sterile right-handed neutrinos ν_R. In general, this phenomena can proceed in three different mechanisms:

1. the helicity change in the neutrino magnetic moment scattering on electrons (or protons and neutrons),
2. the neutrino spin and spin-flavour precession in an external magnetic field, and
3. the neutrino spin and spin-flavour precession in the transversally moving matter currents or in the transversally polarized matter at rest

For completeness note that the important astrophysical consequence of nonzero neutrino millicharges is the neutrino deviation from the rectilinear trajectory. (TO DO: *find out if this is the same thing that IceCube describes in their paper*)

3 Experimental overview

(TO DO: *Create a story for the experimental overview. Point out what is the hole in the current knowledge that NOvA can fill up*)

3.1 Direct muon (anti)neutrino magnetic moment measurements

3.1.1 NOvA (Biao's thesis)

- ν_μ only
- Only comparing total event counts - 25 events observed and 23.78 expected
- Put an upper limit (90% C.L.) of $\mu_{\nu_\mu} < 1.58 \times 10^{-9} \mu_B$ with 10.9% systematic uncertainty on the standard model background
- Used 3.62×10^{20} POT of data (6.74×10^{23} POT for MC) with $T\theta^2 < 0.003\text{GeV} \times \text{Rad}^2$, $0.3 < T < 0.9\text{GeV}$
- Systematic uncertainties estimated with their own studies, instead of using NOvA systematics
  - 12.5% uncertainty on the νMM (for $\mu_\nu = 10^{-9}\mu_B$) and 10.9% for the total SM background
  - Mainly "Low T cutoff" (6.8% and 4.6%), $T\theta^2$ cut (7.1% and 6.9%), Birks B modelling (4.6% and 1.8%) and Parent π^+ in FLUKA (5.9% for both)
  - DOI:10.2172/1418139

3.1.2 MiniBooNE

- ν_μ only
- Observed excess of events (seems a bit too high)
- Thesis

3.1.3 E734 at the Alternating Gradient Synchrotron (AGS) of the Brookhaven National Laboratory

- **Both ν_μ and $\overline{\nu}_\mu$**
- $\mu_{\nu_\mu} < 8.5 \times 10^{-10} \mu_B$
- DOI:10.1103/PhysRevD.41.3297

3.1.4 LSND

3.2 Direct electron (anti)neutrino magnetic moment measurements

3.3 Solar neutrino magnetic moment measurements

3.3.1 XENONnT

First results published in arXiv:2207.11330[5] on 22 July 2022.

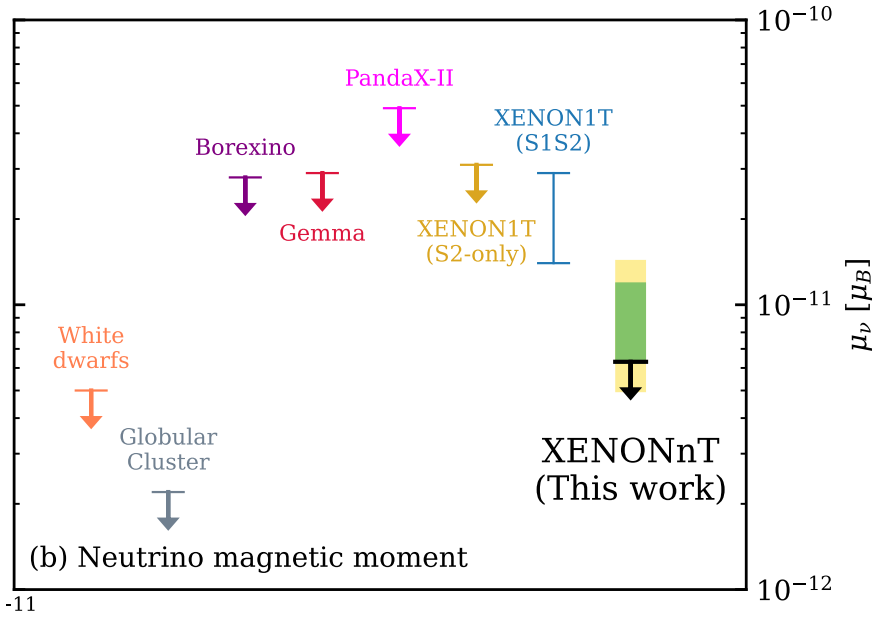

Figure 6: 90% C.L. upper limit on solar neutrinos with an enhanced magnetic moment.

- 5.9 tonne dual-phase liquid xenon TPC dark matter detector
- Region Of Interest is (1,140) keV
- Very low background (5 times lower than XENON1T)
- Tritium excluded as the potential background (also in XENON1T)
- No excess found - XENON1T excess excluded with 4σ
- The 90% C.L. upper limit on solar neutrinos with an "enhanced" magnetic moment is $\mu_{\nu_{sol}} < 6.3 \times 10^{-12}\mu_B$, the strongest non-astronomical limit so far (see fig.6)

Amir Khan used[6] XENONnT's results and derived limits on electromagnetic properties for the three SM neutrino flavours (see fig.7). For ν_μ they

3.3.2 XENON1T

3.3.3 BOREXINO

Should be $\mu_{\nu_e} < 2.8 \times 10^{-11}\mu_B$ [BorexinoLimit2017.pdf]

3.3.4 GEMMA

Should be $\mu_{\nu\ Eff} < 2.9 \times 10^{-11}\mu_B$. [GemmaLimits2013.pdf]

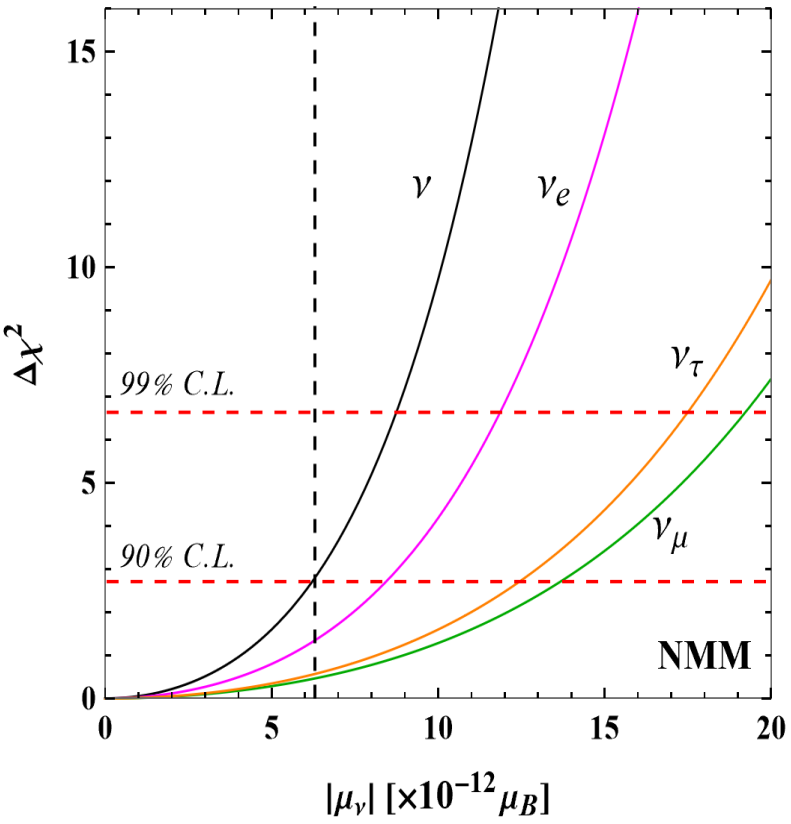

Figure 7: One-dimensional $\Delta\chi^2$ distribution with 90% and 99% C.L. boundaries of neutrino magnetic moments. The distribution in black corresponds to the effective flavor independent magnetic moment

3.4 Other

3.4.1 LHC Forward Physics Facilities

Preliminary sensitivity studies for future experiments (namely for FLArE and FASERν2)

- LHC's Forward Physics Facilities study high energy (TeV) neutrinos of all flavours from the ATLAS interaction point.
- Large opportunity to study tau neutrinos in more detail

3.5 Astrophysics

[NuMMBasicsAndAstro_2022.pdf] Neutrino electromagnetic processes that could be studied/observed in astrophysics

- Neutrino radiative decay
  - Decay of heavier neutrino flavour into a lighter neutrino and a photon
  - "The neutrino radiative decay has been constrained from the absence of decay photons in studies of the solar, supernova and reactor (anti)neutrino fluxes, as well as of the spectral distortions of the cosmic microwave background radiation."
  - Less stringent than the plasmon decay into a nu-antinu pairs
- Plasmon decay to neutrino-antineutrino pair
  - "For constraining neutrino electromagnetic properties, and obtaining upper bounds on neutrino magnetic moments in particular, the most interesting process is the plasmon decay into a neutrino-antineutrino pair [11]"
  - Plasmon decay frees the energy from the stars plasma in form of neutrinos that escape and therefore speeds up the star cooling
  - "observed properties of globular cluster stars provides new upper bounds on the effective neutrino magnetic moment $\mu_{ef} \leq (1.2-2.6)\times 10^{-12}\mu_B$ that is valid for both cases of Dirac and Majorana neutrinos."
- Transition of neutrino helicities $\nu_L \rightarrow \nu_R$ from active to sterile neutrinos
  - Supernovas would cool much faster - not observed for 1987A by Kamioka II and IMB, constraining Dirac neutrino mag. moment

4 Analysis overview

In this analysis we are searching for a signal of possible neutrino magnetic moment events in the NOvA Near Detector. This signal would manifest as an excess of neutrino-on-electron elastic scattering (ν-on-e) events at low electron recoil energies on top of the Standard Model background, as described in Sec. 2.3. In case we would not observe any excess (null hypothesis), we would provide an upper limit on the effective muon neutrino magnetic moment.

The ν-on-e interactions are also used in the Near Detector (ND) group's analysis to constraint the neutrino beam prediction [7], which relies on the precise theoretical knowledge of the ν-on-e interaction cross section. They compare the total number of recorded ν-on-e interactions, with background subtracted based on a data/MC comparison in a sideband region, to the prediction. Since the number of ν-on-e events should only depend on the normalization of the neutrino beam, this analysis should give us a precise validation, or correction, of the neutrino flux normalization. There has been a large amount of work going into this analysis, including making special samples, weights, event classifiers, developing a dedicated event selection, or developing a background subtraction method, among others. To save time and analysis effort, we have taken most of these work at face value and applied it to the neutrino magnetic moment analysis. This will help us get the first good estimate of NOvA's capabilities to constraint (or measure) the neutrino magnetic moment.

The same detector signature of a single forward going electron shower, as present in the ν-on-e events, is also present in the Light Dark Matter (LDM) analysis [8]. This analysis is using a similar event selection to select the LDM events as the ND group, only without the final $E\theta^2$ cut (see Sec.4.3). However, instead of simply comparing the total event counts, the LDM analysis is using a CAFAna-based fitting framework to fit for the possible LDM signal in a distribution of electron recoil energy multiplied by electron recoil angle squared.

Our analysis strategy is to compare the recorded number of neutrino events in data with a predicted number of signal events, which depends on the neutrino magnetic moment value, on top of a Standard Model background. We use the ND group's sideband region to constraint the non-ν-on-e background with data. It is also possible to use a second sideband sample, based on the electron recoil energy, to provide an additional constraint on the ν-on-e background, but this idea has not been visited yet.

In the future, this analysis can be improved for example by improving the event selection, creating additional background samples, by including antineutrino events, or by using using a fit to the energy distribution, similarly to the LDM analysis.

This section describes the simulation samples used to predict the number of signal and background events (Sec.4.1), the weights used to correct for known limitations of the simulation (Sec. 4.2), the event selection used to constraint the background (Sec. 4.3), and the resolution of the electron recoil energy and angle (Sec. 4.4).

4.1 Datasets and Event Reconstruction details

For this analysis we are using near detector CAF samples with the standard Production 5.1 reconstruction.

The SAMWEB definition for the data sample is:

`prod_caf_R20-11-25-prod5.1reco.l_nd_numi_fhc_full_v1_goodruns.`

We are following the standard data blinding procedure and have not looked at any data events until the analysis passes the full collaboration review. The Near Detector group has validated (TO DO: *Figure out where did Yiwen and Wenjie actually look at the data*) using this data sample.

The exposure of the data sample is approximately 1.3848600×10^{21} POT. This is the exposure we use for all the following studies shown in this technical note. The Prod5.1 ND data sample contains data from run 10391 in epoch1a (2014-08-22 21:08:40) until run 14010 in epoch 11a (2021-02-03 15:48:21) (from the period and epoch naming wiki page https://cdcvs.fnal.gov/redmine/projects/novaart/wik

(TO DO: *Briefly describe the MC details. Versions of the individual simulation software*) To tackle the low number of ν-on-e and ν_eCC MEC events in the nominal simulation sample we are using a suit of nominal and enhanced simulation samples for four different signal and background components. Each one contains its nominal sample and special systematically shifted samples for the detector systematics. The use of the samples is summarised in table 6 and described in detail below.

The GENIE tune is `GENIE N1810j 02 11a` (from the Prod5.Frankenstein docdb: 53360). The Genie release used for this production is R20-08-06-prod5.1genie.h, which has GENIE version V3.0.6 [9]

Also prod5.1 uses Geant4 v4.10.4.p02 [10]

We use the standard NOvA simulation (reference NOvA 3fl paper DOI: 10.1103/PhysRevD.106.032004)

Describe how did we deal with the GENIE skew fix. It was the GSF weights that forces "us" to treat the nueCC MEC background differently than the other background. As I understand it, the GSF is applied simply as the new weight. No change to the systematics is required.

Reference: A. Mislivic, “Genie skew reweight validation.” NOvA Internal Document, DocDB: 553811 [from antinueCC IncXSec docdb:53691] "Final state kinematics were predicted by the N1810j 00 000 tune, but total cross section were generated with the intended N1810j 0211a179 tune, which differed in RES and DIS rates tuned to external data. Properly correcting the skew180 would require all simulation to be regenerated, so a temporary solution developed by the NOvA181 Cross-section Tuning Group involves reweighing production 5.1 events to the default N1810j 00 000.182 An additional modification to the GENIE MEC contribution are applied to better agree with NOvA183 ND data.

MC includes simulation in the rock surrounding the ND

(TO DO: *Describe here that we’re using the nominal ND MC sample for signal utilizing the simple relationship between the Standard Model cross section and the neutrino magnetic moment cross section (ref. theory)*)

The signal of the neutrino magnetic moment analysis is just a re-weighted signal of the ν-on-e analysis from the near detector group. We are using the same event selection as the near detector group.

(TO DO: *Say already here that the POT inside the enhanced MC samples are not properly accounted for in CAFAna (Loader issue) and so the event counts need to be adjusted post-hoc*)

Table 1: Overview of the simulation samples corresponding to different signal and background components.

Signal	Enhanced ν-on-e sample
ν-on-e background	Enhanced ν-on-e sample
ν_eCC MEC background	Enhanced ν_eCC MEC sample
Other background	Nominal ND CAF sample

Enhanced ν-on-e sample

(TO DO: *Describe the nuone sample*) Created by Wenjie Wu (was it just him or also Yiwen?) to do ... and fully described in the technote [7]. Using the overlayed and filematched samples for consistency.

Incorrect POT is 3.6995434e+20, Correct POT is 1.7209423e+24 (this should be filematched)

(TO DO: *Find a reference and reasoning for why Wenjie hasn't created the other systematics samples*) We only have the selected few systematics definitions because ...

(TO DO: *Describe the differences*)

- Missing cross section parameters - unable to use cross section weights or so
- Special mode for nu-on-e elastic scattering 10005

The list of the nu-on-e sample definitions is in table 2.

Enhanced ν_eCC MEC sample

Created by Yiwen Xiao [7] to tackle the low statistics of the ν_eCC MEC background events and subsequently large and unphysical cross section weights.

Incorrect POT is 4.7334120e+23 and correct POT is 1.9880340e+24. This is filematched

(TO DO: *List the limitations of the sample in the q3-q0 parameter space*)

Near Detector filematched CAF sample

(TO DO: *describe all the ND nominal CAF samples*) (TO DO: *Also mention the decaf sample and discuss if we could use them or not*)

The nominal ND MC includes 4x data POT. The systematics are file-matched to remove any statistical bias

Total POT is 5.54497e+21 But for the filematched samples (batch 2) there's only 1.93109e+21

4.2 Analysis weights

(TO DO: *Describe why do we use weights*) What are the weights we are using and why?

Table 2: SAMWEB definitions for the enhanced ν-on-e samples.

Nominal:

`prod_caf_R20-11-25-prod5.1reco.g_nd_genie_N1810j0211a_nonswap_fhc_nova_v08_full_v1_nuone_overlay`

Systematically shifted samples:

`prod_caf_R20-11-25-prod5.1reco.g_nd_genie_N1810j0211a_nonswap_fhc_nova_v08_full_calibup_v1_nuone_overlay`

`prod_caf_R20-11-25-prod5.1reco.g_nd_genie_N1810j0211a_nonswap_fhc_nova_v08_full_calibdown_v1_nuone_overlay`

`prod_caf_R20-11-25-prod5.1reco.g_nd_genie_N1810j0211a_nonswap_fhc_nova_v08_full_ckvup_v1_nuone_overlay`

`prod_caf_R20-11-25-prod5.1reco.g_nd_genie_N1810j0211a_nonswap_fhc_nova_v08_full_ckvdown_v1_nuone_overlay`

`prod_caf_R20-11-25-prod5.1reco.g_nd_genie_N1810j0211a_nonswap_fhc_nova_v08_full_lightlevelup_v1_nuone_overlay`

`prod_caf_R20-11-25-prod5.1reco.g_nd_genie_N1810j0211a_nonswap_fhc_nova_v08_full_lightleveldown_v1_nuone_overlay`

Table 3: SAMWEB definitions of the ν_eCC MEC background sample.

Nominal:

`YiwenXiao_NueCCMEC_Single_NJobs7500_CAF_NonSwap_filematch`

Systematically shifted samples:

`YiwenXiao_NueCCMEC_Single_NJobs7500_CAF_NonSwap_CalibUp_Combined_240124_filematch`

`YiwenXiao_NueCCMEC_Single_NJobs7500_CAF_NonSwap_CalibDown_Combined_240124_filematch`

`YiwenXiao_NueCCMEC_Single_NJobs7500_CAF_NonSwap_CkvUp_Combined_240124_filematch`

`YiwenXiao_NueCCMEC_Single_NJobs7500_CAF_NonSwap_CkvDown_Combined_240124_filematch`

`YiwenXiao_NueCCMEC_Single_NJobs7500_CAF_NonSwap_LLUp_Combined_240124_filematch`

`YiwenXiao_NueCCMEC_Single_NJobs7500_CAF_NonSwap_LLDown_Combined_240124_filematch`

`YiwenXiao_NueCCMEC_Single_NJobs7500_CAF_NonSwap_Aging_Combined_240124_filematch`

`YiwenXiao_NueCCMEC_Single_NJobs7500_CAF_NonSwap_CalibShape_Combined_240124_filematch`

`YiwenXiao_NueCCMEC_Single_NJobs7500_CAF_NonSwap_MCNP_Combined_240124_filematch`

Table 4: SAMWEB definitions of the other background samples.

Nominal:

`prod_caf_R20-11-25-prod5.1reco.a_nd_genie_N1810j0211a_nonswap_fhc_nova_v08_full_v1`

Systematically shifted samples:

`prod_caf_R20-11-25-prod5.1reco.e_nd_genie_N1810j0211a_nonswap_fhc_nova_v08_full_calibup_v1_batch2`

`prod_caf_R20-11-25-prod5.1reco.e_nd_genie_N1810j0211a_nonswap_fhc_nova_v08_full_calibdown_v1_batch2`

`prod_caf_R20-11-25-prod5.1reco.f_nd_genie_N1810j0211a_nonswap_fhc_nova_v08_full_ckvup_v1_batch2`

`prod_caf_R20-11-25-prod5.1reco.f_nd_genie_N1810j0211a_nonswap_fhc_nova_v08_full_ckvdown_v1_batch2`

`prod_caf_R20-11-25-prod5.1reco.g_nd_genie_N1810j0211a_nonswap_fhc_nova_v08_full_lightlevelup_v1_batch2`

`prod_caf_R20-11-25-prod5.1reco.g_nd_genie_N1810j0211a_nonswap_fhc_nova_v08_full_lightlevelup_v1_batch2`

`prod_caf_R20-11-25-prod5.1reco.f_nd_genie_N1810j0211a_nonswap_fhc_nova_v08_full_detectorageing_v1_batch2`

`prod_caf_R20-11-25-prod5.1reco.f_nd_genie_N1810j0211a_nonswap_fhc_nova_v08_full_calibshape_v1_batch2`

`prod_caf_R20-11-25-prod5.1reco.g_nd_genie_N1810j0211a_nonswap_fhc_nova_v08_full_mcnp_v1_batch2`

To correct for known deficiencies in simulation of neutrino flux or cross sections we apply weights calculated for each event.

Table 5 shows what CAFAna weights are used to simulate what signal/background sample.

Table 5: Overview of CAFAna weights applied to each analysis sample.

Signal	Flux and neutrino magnetic moment weights
ν-on-e background	Flux and radiative correction weights
ν_eCC MEC background	Flux and cross section weights
Other background	Flux and cross section weights

PPFX weight

`ana::kPPFXFluxCVWgt` [11] (TO DO: *What does this do (one sentence ish).*) Maybe cite Leo's thesis? Or paper? L. Aliaga, "Neutrino Flux Prediction for the NuMI Beamline." PhD Thesis, FERMILAB-1081 THESIS-2016-03

Prod5.1 GSF XSec weight

`ana::kXSecCVWgt2020GSFProd51` (TO DO: *Find the reference: possibly Maria's docdb:53336 together with the official 2020 XSec tuning technote docdb:43962.*)

NOvAReweight reference: J. Wolcott, "NOvARwgt software." https://github.com/novaexperiment/NOvARwg public.

(TO DO: *Briefly describe what does this do. Also mention Yiwen's talk/technote about the large XSec weights that made her create an enhanced nueCC MEC sample.*)

We are only using the for the background since we assume that the cross section for the signal is perfect. Also there are not weights for this kind of interaction.

Radiative correction weight

(TO DO: *Why are we doing this? (reference Yiwen's talk/technote).*)

Mention here where did I get the original GENIE cross section from (reference Yiwen's talk or technote, plus the original paper that was used). nu-on-e technote[7]

(TO DO: *Write out the actual version of the weight. Including the original and the corrected XSec constants*)

MINERvA paper: https://journals.aps.org/prd/pdf/10.1103/PhysRevD.100.092001

Say that we are not using the third part of the correction because it is tiny and it makes no difference. (tried and tested)

(TO DO: *correct the equation*) Calculated as

$$weight_{\text{Radiative Corr.}} = \left.\frac{d\sigma_{\nu-on-e}}{dy}\right|_{\text{Radiative Corr.}} \Big/ \left.\frac{\mathrm{d}\sigma_{\nu-on-e}}{\mathrm{d}y}\right|_{\text{GENIE 3}} ; y = \frac{E_e - m_e}{E_\nu} \tag{34}$$

Neutrino magnetic moment signal as a weight

(TO DO: *What does this do and why does it work? Reference the theory part as to why is the magnetic moment signal simply a rescaling of the GENIE cross section.*)

Using the same tree-level cross section from GENIE as in the rad. corr. weight.

(TO DO: *Write the name of the weight in CAFAna/nuone namespace and where it is located*)

(TO DO: *correct the equation*) Calculated as

$$weight_{\nu\text{ Mag. Moment}} = \left.\frac{d\sigma_{\nu-on-e}}{dy}\right|_{\nu\text{ Mag. Moment}} \Big/ \left.\frac{\mathrm{d}\sigma_{\nu-on-e}}{\mathrm{d}y}\right|_{\text{GENIE 3}} ; y = \frac{E_e - m_e}{E_\nu} \tag{35}$$

4.3 Event selection

We are trying to select low energy neutrino-on-electron events, which are characterised by a single very forward going electron shower. Since these are the same events as are used in the Near Detector group's analysis to constraint the neutrino beam prediction with a neutrino-on-electron events [7], we have taken taken their event selection without changes. This is to save time and analysis efforts, but also to get a first good estimation of NOvA's capabilities to constraint (or measure) neutrino magnetic moment. Almost the same selection is also used in the Light Dark Matter analysis [8], only without the final $E\theta^2$ cut.

We explain the motivation behind each cut of the event selection and discuss their effect on the neutrino magnetic moment events below. We also consider possible improvements to the event selection for a future (re-)analysis.

The code to make plots and analyse the event selection is located in the `NuMagMomentAna/NuMMAnalysis/EventSelection` directory. The signal definition is in `NuoneCuts.h` and the cut values in the `EventCVNCuts.h/cxx` scripts from the `NuMagMomentAna/Cuts` directory.

Signal definition

To define the signal and background samples we use the true information listed in table 6. The neutrino magnetic moment signal definition is the same as the neutrino-on-electron background with the neutrino magnetic moment weight applied, as explained in sec.4.2.

The signal definitions use the *kMode* variable instead of the *kIntType*, which is now deprecated (ref.: various Slack conversations). Mode 10005 denotes only the ν-on-e events and is only available for the enhanced ν-on-e samples, while mode 5 denotes all electron scattering events, including inverse muon decay interactions. That is why we had to add a requirement of an electron in the final state. Mode 10 denotes all Meson Exchange Current (MEC) events.

We are using the ND group's [7] signal definition including a requirement for the true vertex to lie within their fiducial volume (defined below). This is the cut name `NDNuoneFiducial`. This is in contrast with the LDM analysis [8], which uses the `ana::kVtxIsContained` cut instead, which has a looser boundary. This choice has only a negligible effect on the final number of selected events and only affects the selection efficiency.

Table 6: Overview of signal and background definitions.

Signal	`kMode== 10005 && NDNuoneFiducial`
ν-on-e background	`kMode== 10005 && NDNuoneFiducial`
ν_eCC MEC background	`!(kMode== 5 && kElInFinState && NDNuoneFiducial) && (kIsCC && kIsNue && kMode == 10)`
Other background	`!(kMode== 5 && kElInFinState && NDNuoneFiducial) && !(kIsCC && kIsNue && kMode == 10)`

Pre-selection

The pre-selection cuts have been kept from the ν_eCC analysis with loosened cut values (TO DO: *find a reference for this analysis*). Pre-selection cuts include basic quality cuts that remove events with invalid vertex reconstruction and events with no reconstructed prongs, as shown on Fig. 8. They also remove the obvious ν_μCC interactions by requiring that the length of the longest prong is < 800 cm, number of planes crossed by the longest prong is < 120, and the summed number of cells for all prongs in the slice is < 600. In pre-selection we also include a cut on the time difference between the mean times of the "current" slice and of the slice closest in time, which should be > 25 ns. This ensures that ... (TO DO: *describe why do we need the closest slice cut with reference to Yiwen's talk and technote*). Relative comparison of signal, ν-on-e background, and other background distributions for the pre-selection variables is shown on Fig. 9.

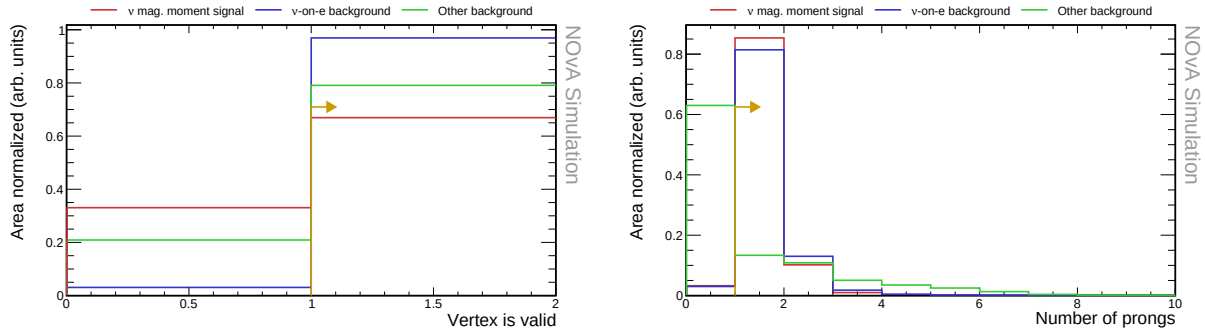

Figure 8: Relative comparison of signal, ν-on-e background, and other background events for basic pre-selection variables. No cuts were applied to make these plots. Gold lines show the cut values for the shown variables.

Fiducial and containment cuts

(TO DO: *Describe what does the fiducial cut do*) We require that the reconstructed vertex is contained within the following volume: $-185 < \mathrm{Vtx}_X < 175, -175 < \mathrm{Vtx}_Y < 175, 95 < \mathrm{Vtx}_Z < 1095$ cm.

To ensure all the energy is contained within the detector and to remove events originating outside of the detector (rock muons), we require that the extreme positions of hits for all prongs in the slice are within the following volume: $-190 < \mathrm{min}_X, \mathrm{max}_X < 180, -180 < \mathrm{min}_Y, \mathrm{max}_Y < 190, 105 < \mathrm{min}_Z, \mathrm{max}_Z < 1275$ cm.

Single particle requirement

To selection events with a single particle we require that the fraction of energy contained in the most energetic shower is > 0.8, that the summed energy of all cells (above threshold and within ± 8 planes from the vertex) outside of the most energetic shower is < 0.02 GeV, and that the distance between the vertex and the start of the primary shower is < 20 cm.

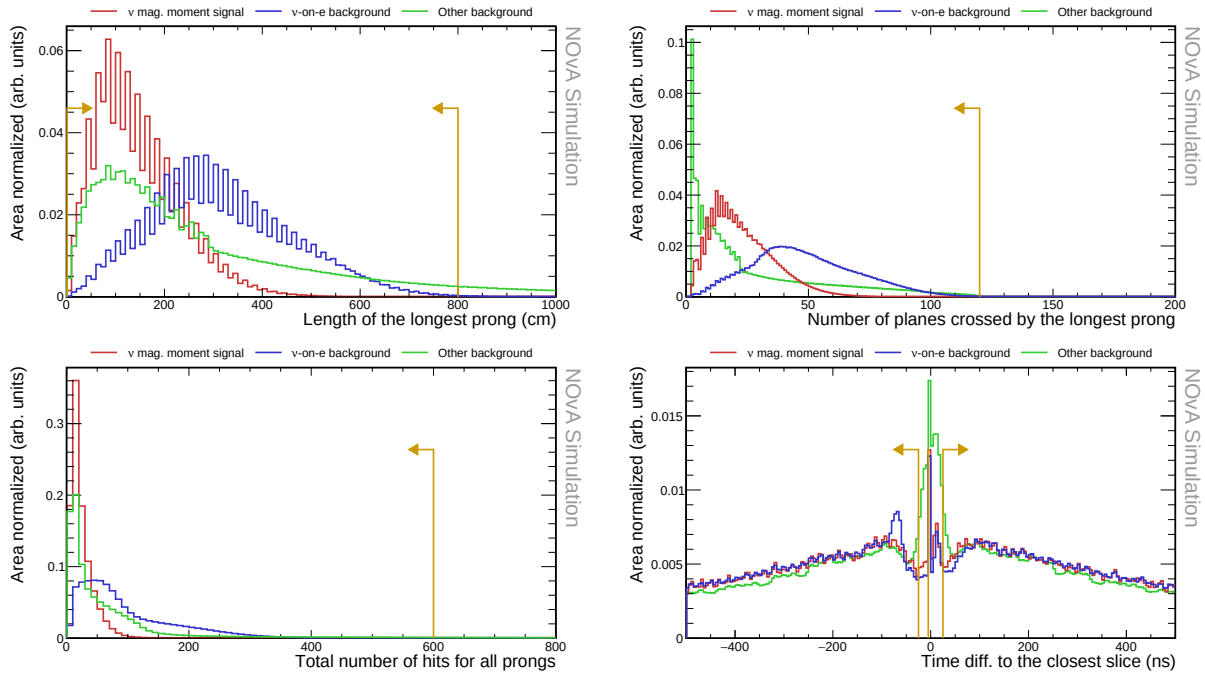

Figure 9: Relative comparison of signal, ν-on-e background, and other background events for pre-selection variables. Cuts on VtxIsValid and number of prongs were applied to make these plots. Gold lines show the cut values for the shown variables.

Shower energy cut

(TO DO: *discuss the energy cut, should this be removed? What is the effect on the event count? Why was this included in the first place (the identifiers are not as strong for lowere energies - is this true though? - also there are further unexplored backgrounds that would need to be further studied and explore. Maybe depends on where would we move the cut...)*) The calorimetric energy of the primary shower is required to be within $0.5 < E_{cal} < 5$ GeV.

Event classifiers

We are using two event classifiers based on convolution neural network that were developed specifically to identify ν-on-e interactions. The first one (`NuoneID`) is trained to select ν-on-e events and the second one (`Epi0ID`) is trained on the events passing the `NuoneID` to reject the π^0 background. Our selection requires that `NuoneID`> 0.73 and that `Epi0ID`> 0.92.

(TO DO: *reference theory for the kinematics of nuone scattering*) We require that the product of reconstructed energy of the primary shower and the square of its angle from the Z axis is $E_{cal}\theta^2 < 0.005$ GeV $\times$ rad^2.

(TO DO: *Add plots of distributions of the event selection variables with two columns. LHS shows no cuts applied and RHS shows all previous cuts applied*)

Using the many plots below that show the effect of each of the cuts on the signal and all

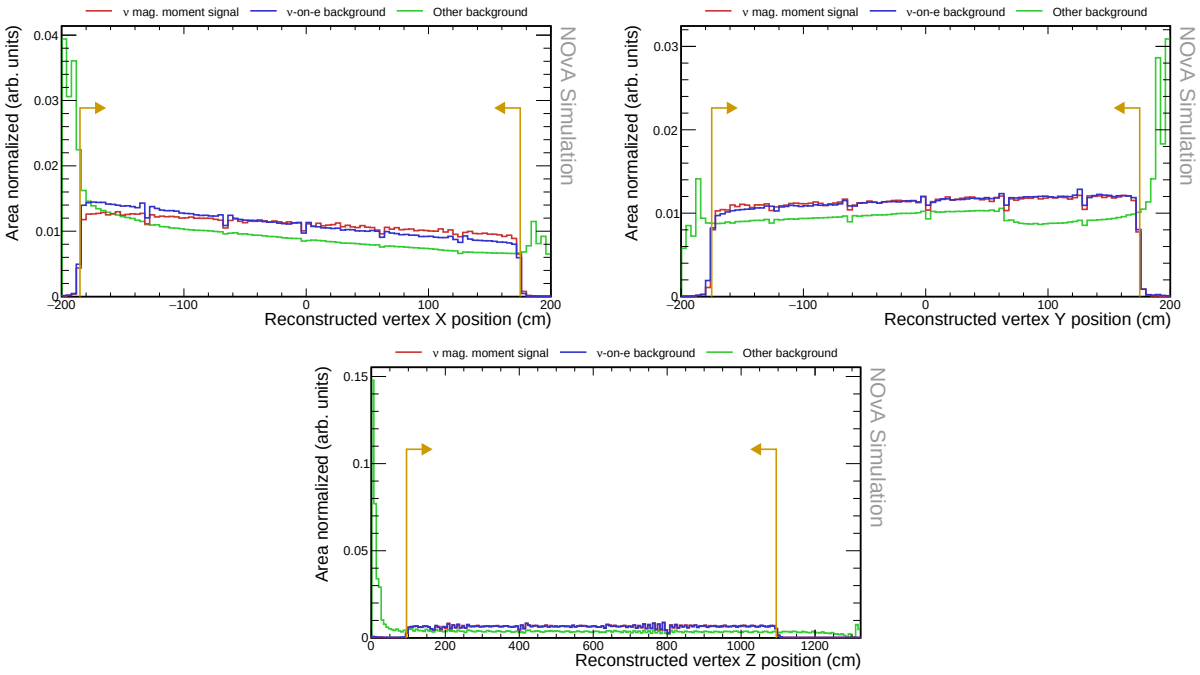

Figure 10: Relative comparison of signal, ν-on-e background, and other background events for the reconstructed vertex. No cuts were applied to make these plots. Gold lines show the cut values that create the fiducial volume.

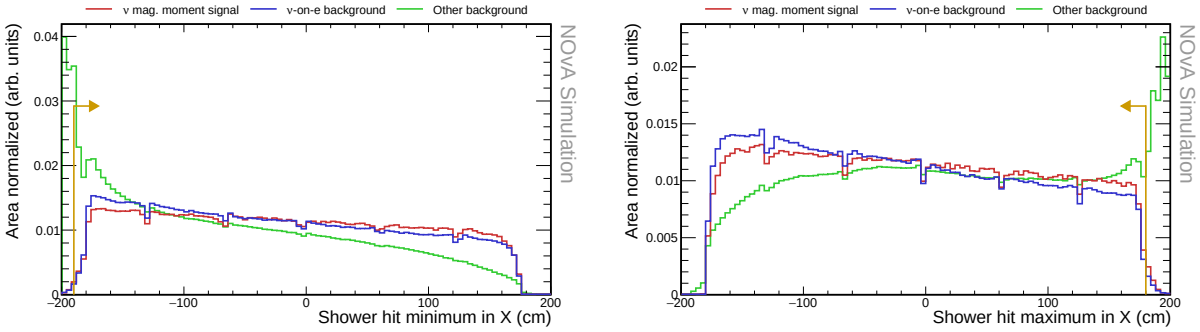

Figure 11: Relative comparison of signal, ν-on-e background, and other background events for the minimum and maximum position of the reconstructed shower along the X axis. Pre-selection and fiducial cuts were applied to make these plots. Gold lines show the values of the containment cuts.

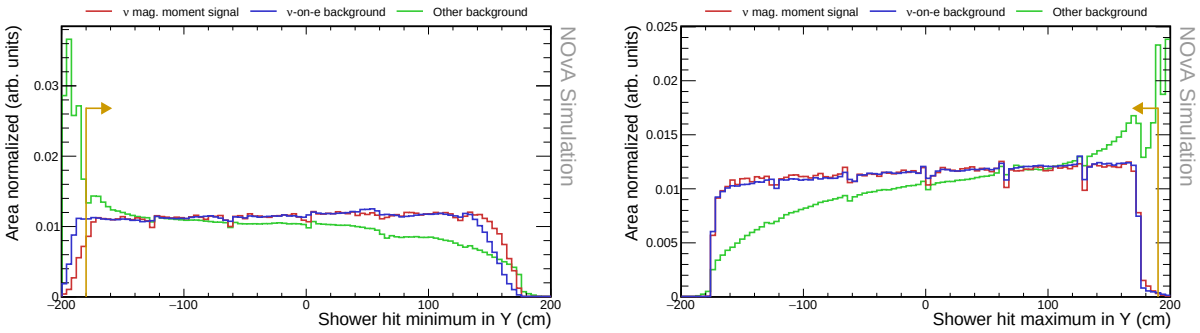

Figure 12: Relative comparison of signal, ν-on-e background, and other background events for the minimum and maximum position of the reconstructed shower along the Y axis. Pre-selection and fiducial cuts were applied to make these plots. Gold lines show the values of the containment cuts.

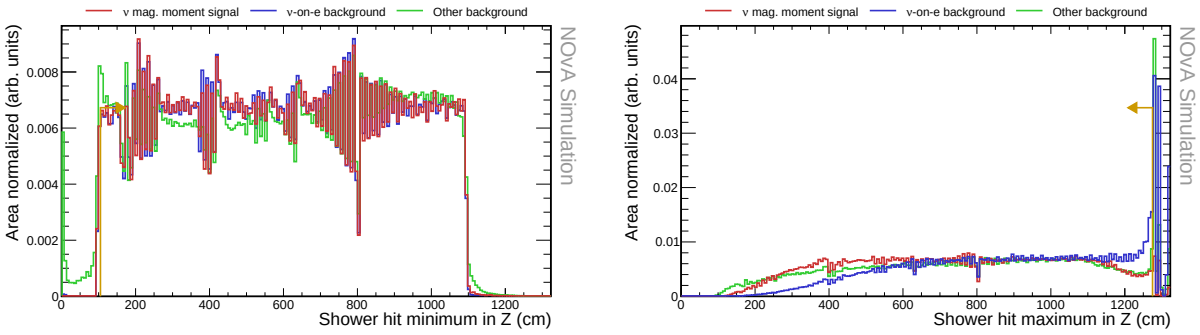

Figure 13: Relative comparison of signal, ν-on-e background, and other background events for the minimum and maximum position of the reconstructed shower along the Z axis. Pre-selection and fiducial cuts were applied to make these plots. Gold lines show the values of the containment cuts.

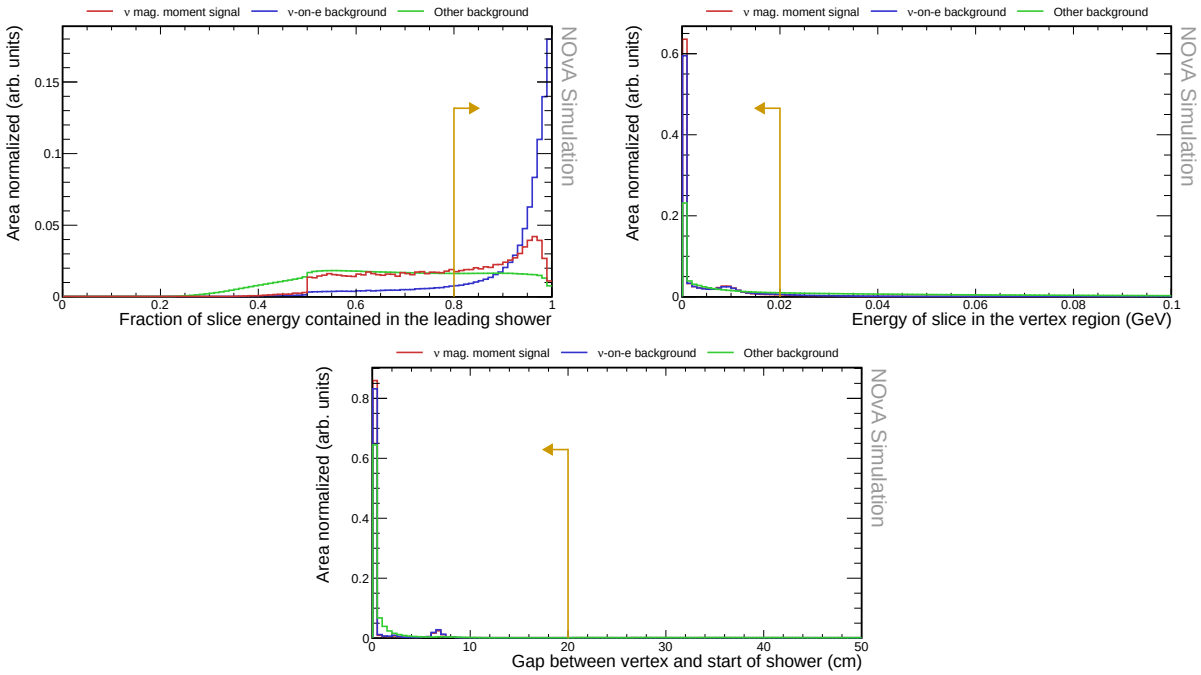

Figure 14: Relative comparison of signal, ν-on-e background, and other background events for the reconstructed vertex. No cuts were applied to make these plots. Gold lines show the cut values that create the fiducial volume.

background events. (For signal we are showing NuMM=...)

(TO DO: *Describe the cutflow tables below*) The final event count and efficiency of each of the cuts is shown on the table 7. Table 16 shows the dissemination of background into the individual components.

(TO DO: *Add a discussion of possible improvements on the event selection on its limitations - mostly for the analysis review committee*) From here we can see that ... Maybe what can be improved is... This can likely be improved upon by specifically selection low energy events and removing the cut on the reconstructed shower energy.

4.4 Resolution and binning

(TO DO: *Add the energy resolution and binning plots*) The electron energy and angle distributions and resolutions. Are we going to fit in E, Th, or ETh2? Is there something else?

Show plots of Reco V True for both energy and angle. (Should I show it with or without the energy cut?). Also show the resolution plots.

4.5 Systematic uncertainties

(TO DO: *Describe the main systematic uncertainties. Add plots showing their effect on the NuMM events. Possibly with different event selection variables as X axes. Also show the final table with the*

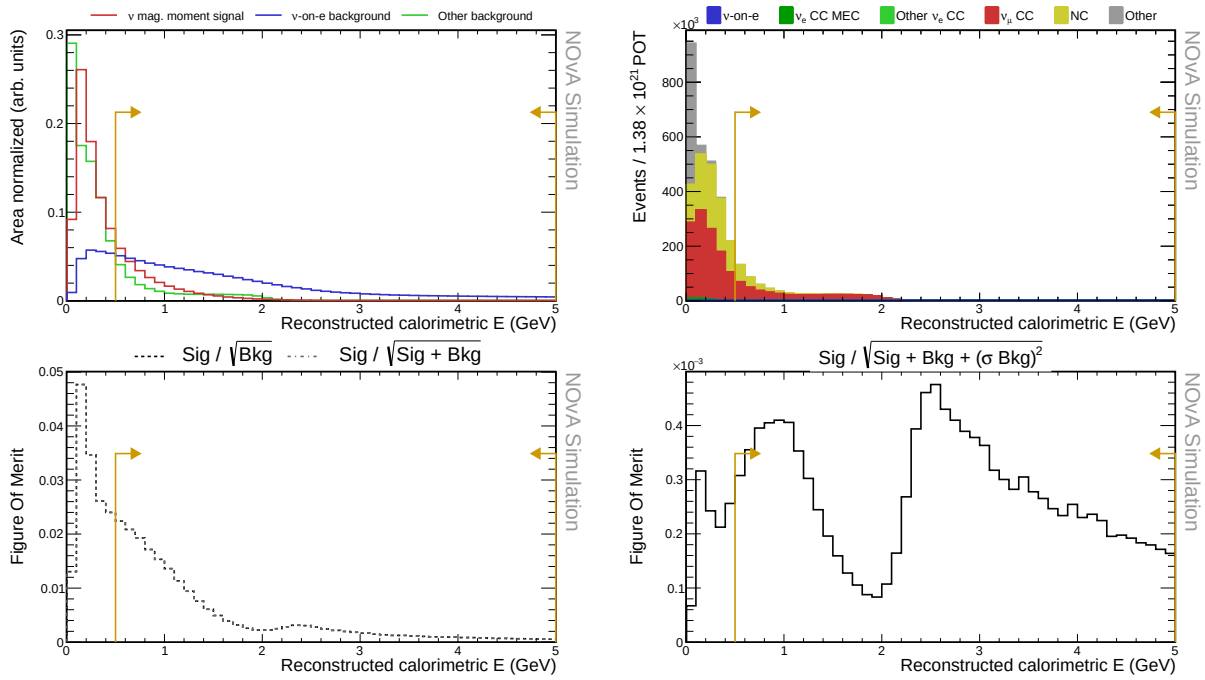

Figure 15: Relative comparison of signal, ν-on-e background, and other background events for the reconstructed vertex. No cuts were applied to make these plots. Gold lines show the cut values that create the fiducial volume.

percentages summed) Plots showing combined uncertainties for signal and backgrounds. Maybe also some interpolations. Table of systematic uncertainties on the event count.

Normalization systematics

(TO DO: *Describe the normalization systematics (or just remove this if not using them in the end*) Should we include normalization systematics? Would that make any difference? There's a POT scaling uncertainty which is very small (find out exactly how small).

In the fitting experiment normalization uncertainties would probably not make any difference whatsoever, but in the counting experiment they might be important?

Neutrino flux systematics

(TO DO: *Describe the flux uncertainties. Describe the PCA. Describe the difference between what the ND group is doing and what we're doing*) Using the PCA vs using the PPFX universes+beam transport separately. Plots of energy showing shifts for signal and backgrounds separately

(TO DO: *understand differences with ND and 3F methods*)

This is mainly a normalization. Discuss how to use the fact that ν-on-e events can be used (and are used) to constraint the beam uncertainty. Would the counting experiment still be valid then? Maybe if we made another sideband sample...

Detector systematics

(TO DO: *Make plots of energy showing shifts for signal and backgrounds separately*) Reference for the Prod5.1 detector systematics is docdb 53225

Cross section systematics

(TO DO: *Describe the XSec systs*) Only for the non nu-on-e background. Assuming the nu-on-e events (including the signal events) are precisely known.

Plots of energy showing shifts for signal and backgrounds separately

4.6 Fitting framework

(TO DO: *Describe the fitting framework, ideally with an example plot, maybe with some arrows*) How does the fitting framework work? It's based on the framework developed by Mu Wei for the Light Dark Matter analysis (ref.) which was developed together (is this fair?). Basic description of the framework.

Also this framework is used for both LDM and NuMM together. It is trivial to simply switch between including the NuMM or LDM in it. This was done to save space in creating predictions

Table 7: Event selection cutflow table

Selection	**ν Mag. Moment signal**			**ν-on-e background**			**Other background**		
	N_{sig}	ε^{N-1}	$\varepsilon\,(\%)$	N_{IBkg}	ε^{N-1}	$\varepsilon\,(\%)$	N_{Bkg}	ε^{N-1}	$\varepsilon\,(\%)$
No Cut	269.77	100	100	3.43×10^{3}	100	100	2.96×10^{8}	100	100
Vtx Is Valid	180.58	66.94	66.94	3.33×10^{3}	96.94	96.94	2.34×10^{8}	79.09	79.09
N Prongs	174.69	96.74	64.76	3.23×10^{3}	96.99	94.02	8.66×10^{7}	37.00	29.27
Png Length	174.67	99.99	64.75	3.22×10^{3}	99.64	93.68	7.67×10^{7}	88.56	25.92
N Planes	174.67	100	64.75	3.22×10^{3}	99.98	93.67	7.67×10^{7}	99.98	25.92
N Cells	174.67	100	64.75	3.22×10^{3}	99.98	93.65	7.42×10^{7}	96.78	25.08
Closest Slc	169.82	97.22	62.95	3.14×10^{3}	97.54	91.35	6.95×10^{7}	93.68	23.49
Fiducial	167.72	98.76	62.17	3.09×10^{3}	98.41	89.89	3.59×10^{7}	51.71	12.15
Cont.	159.37	95.02	59.08	2.48×10^{3}	80.43	72.30	1.38×10^{7}	38.35	4.66
ShwE Frac.	150.37	94.35	55.74	2.42×10^{3}	97.59	70.56	8.82×10^{6}	63.97	2.98
Vtx E	142.29	94.63	52.74	2.18×10^{3}	90.16	63.62	4.15×10^{6}	47.07	1.40
Shw Gap	137.96	96.96	51.14	2.09×10^{3}	95.58	60.80	3.25×10^{6}	78.34	1.10
Shw E	37.13	26.92	13.76	1.36×10^{3}	65.10	39.58	6.25×10^{5}	19.21	0.21
Nuoneid	29.48	79.39	10.93	940.21	69.18	27.38	2.42×10^{4}	3.88	8.19×10^{-3}
Epi0id	22.51	76.35	8.34	749.93	79.76	21.84	1.47×10^{4}	60.75	4.97×10^{-3}
$E\theta^2$	19.74	87.73	7.32	675.02	90.01	19.66	84.15	0.57	2.84×10^{-5}
$E\theta^2$ **(sb)**	2.74	-	1.01	74.30	-	2.16	1.01×10^{3}	-	3.43×10^{-4}
No ShwE	37.62	-	13.94	782.67	-	22.79	238.79	-	8.07E-05

since our backgrounds are exactly the same (or at least they should be...). Theoretically this could be separated into two difference frameworks.

- <NDPredictionSingleElectron> Prediction class which holds the LDM as a special 2-D spectrum (not used for NuMM), and NuMM, ν-on-e background, ν_eCC MEC background and other background as simple 1-D spectra. Also scaling each spectra by...
- <NDPredictionSystSingleElectron> class derived from PredictionInterp that takes in the NDPredictionSingleElectron and applies systematic shifts to it. Includes the interpolation/extrapolation between the systematic shifts.
- FitVariables and what do they do
- Fitter which does exactly what... What are the parameters of the fit? What are the results/outputs?

5 Results / Fake data studies

[to do]: talk about the shape-only versus normalisation-only strategies for the differential versus single-bin analyses.

I think it might be a good idea to talk about this already in the analysis overview section.

I need to also discuss fake data studies. Should I talk about this now? Probably

5.1 Counting experiment

Single bin analysis - total numbers of signal and backgrounds predicted. Possible background corrections and its effect on the background uncertainties.

5.2 Binned experiment

Plots showing delta chi2 for stats and systs separately. Plot showing the chi2 with limits. Maybe talk about using different binning and variables and the effect.

Also need to somehow quantify the various fitter settings, like different seeding values, different range of profiling. Should I talk about Feldman-Cousins?

5.2.1 Sensitivities and limits

6 Conclusion

(TO DO: *Report the limit with its uncertainty*)

(TO DO: *Very briefly discuss differences with current world limit and how the techniques differ*)

(TO DO: *Very briefly summarise expectations for future measurements.*)

References

[1] Carlo Giunti, Julieta Gruszko, Benjamin Jones, Lisa Kaufman, Diana Parno, and Andrea Pocar. Report of the Topical Group on Neutrino Properties for Snowmass 2021. 9 2022. arXiv:2209.03340.

[2] Carlo Giunti and Alexander Studenikin. Neutrino electromagnetic interactions: A window to new physics. *Rev. Mod. Phys.*, 87:531–591, Jun 2015. URL: https://link.aps.org/doi/10.1103/RevModPhys.87.531, doi:10.1103/RevModPhys.87.531.

[3] Nicole F. Bell, Mikhail Gorchtein, Michael J. Ramsey-Musolf, Petr Vogel, and Peng Wang. Model independent bounds on magnetic moments of Majorana neutrinos. *Phys. Lett. B*, 642:377–383, 2006. arXiv:hep-ph/0606248, doi:10.1016/j.physletb.2006.09.055.

[4] P. Vogel and J. Engel. Neutrino electromagnetic form factors. *Phys. Rev. D*, 39:3378–3383, Jun 1989. URL: https://link.aps.org/doi/10.1103/PhysRevD.39.3378, doi:10.1103/PhysRevD.39.3378.

[5] E. Aprile et al. Search for New Physics in Electronic Recoil Data from XENONnT. *Phys. Rev. Lett.*, 129:161805, Oct 2022. URL: https://link.aps.org/doi/10.1103/PhysRevLett.129.161805, arXiv:2207.11330, doi:10.1103/PhysRevLett.129.161805.

[6] Amir N. Khan. Light new physics and neutrino electromagnetic interactions in XENONnT. *Phys. Lett. B*, 837:137650, 2023. arXiv:2208.02144, doi:10.1016/j.physletb.2022.137650.

[7] Wenjie Wu and Yiwen Xiao. Neutrino-Electron Elastic Scattering in the NOvA Near Detector - Technote. NOVA Document 56383, October 2023. NOvA technical note. URL: https://nova-docdb.fnal.gov/cgi-bin/sso/ShowDocument?docid=56383.

[8] Barnali Brahma, Tyler Horoho, and Mu Wei. Technote for Light DM Search using NOvA ND Data. NOVA Document 59439, November 2023. NOvA technical note. URL: https://nova-docdb.fnal.gov/cgi-bin/sso/ShowDocument?docid=59439.

[9] C. Andreopoulos et al. The GENIE Neutrino Monte Carlo Generator. *Nucl. Instrum. Meth. A*, 614:87–104, 2010. arXiv:0905.2517, doi:10.1016/j.nima.2009.12.009.

[10] S. Agostinelli et al. GEANT4–a simulation toolkit. *Nucl. Instrum. Meth. A*, 506:250–303, 2003. doi:10.1016/S0168-9002(03)01368-8.

[11] Leonidas Aliaga Soplin. PPFX tech-note for the 2017 analysis. NOVA Document 23441, November 2017. NOvA technical note. URL: https://nova-docdb.fnal.gov/cgi-bin/sso/ShowDocument?docid=23441.

Figure 16: Event selection cutflow table for background components

Selection	ν_eCC MEC			ν_eCC Other			ν_μCC			NC			Other		
	N	ε^{N-1}	ε (%)	N	ε^{N-1}	ε (%)	N	ε^{N-1}	ε (%)	N	ε^{N-1}	ε (%)	N	ε^{N-1}	ε (%)
No Cut	3.50×10^{4}	100	100	3.23×10^{6}	100	100	2.24×10^{8}	100	100	3.40×10^{7}	100.	100	3.49×10^{7}	100	100
Vtx Is Valid	3.27×10^{4}	93.58	93.58	2.62×10^{6}	81.14	81.14	1.99×10^{8}	89.02	89.02	2.57×10^{7}	75.55	75.55	6.53×10^{6}	18.70	18.70
N Prongs	2.74×10^{4}	83.76	78.39	1.39×10^{6}	53.05	43.05	6.75×10^{7}	33.89	30.17	1.51×10^{7}	58.57	44.25	2.65×10^{6}	40.51	7.58
Png Length	2.73×10^{4}	99.79	78.22	1.37×10^{6}	98.53	42.42	5.77×10^{7}	85.56	25.81	1.49×10^{7}	99.07	43.84	2.64×10^{6}	99.87	7.57
N Planes	2.73×10^{4}	99.99	78.22	1.37×10^{6}	99.99	42.41	5.77×10^{7}	99.98	25.81	1.49×10^{7}	100	43.84	2.64×10^{6}	100	7.57
N Cells	2.73×10^{4}	99.99	78.21	1.28×10^{6}	93.49	39.65	5.59×10^{7}	96.82	24.98	1.44×10^{7}	96.34	42.24	2.64×10^{6}	100	7.57
Closest Slc	2.73×10^{4}	99.79	78.05	1.21×10^{6}	94.25	37.37	5.33×10^{7}	95.40	23.84	1.35×10^{7}	94.17	39.77	1.43×10^{6}	54.22	4.10
Fiducial	1.39×10^{4}	51.12	39.90	6.30×10^{5}	52.10	19.47	2.60×10^{7}	48.77	11.62	8.25×10^{6}	60.99	24.26	1.05×10^{6}	73.53	3.02
Cont.	9.32×10^{3}	66.82	26.66	2.63×10^{5}	41.72	8.12	7.64×10^{6}	29.38	3.42	4.96×10^{6}	60.15	14.59	9.12×10^{5}	86.62	2.61
ShwE Frac.	9.20×10^{3}	98.70	26.32	1.95×10^{5}	74.39	6.04	4.82×10^{6}	63.10	2.15	2.97×10^{6}	59.78	8.72	8.28×10^{5}	90.81	2.37
Vtx E	5.92×10^{3}	64.33	16.93	6.05×10^{4}	30.96	1.87	1.97×10^{6}	40.79	0.88	1.36×10^{6}	45.75	3.99	7.62×10^{5}	92.03	2.18
Shw Gap	5.50×10^{3}	92.91	15.73	4.62×10^{4}	76.40	1.43	1.58×10^{6}	80.18	0.70	1.06×10^{6}	77.78	3.10	5.69×10^{5}	74.61	1.63
Shw E	3.62×10^{3}	65.81	10.35	1.12×10^{4}	24.15	0.35	4.38×10^{5}	27.80	0.20	1.71×10^{5}	16.15	0.50	1.28×10^{3}	0.23	3.68×10^{-3}
Nuoneid	1.40×10^{3}	38.63	4.00	2.11×10^{3}	18.89	0.065	1.17×10^{4}	2.66	5.21×10^{-3}	8.99×10^{3}	5.27	0.026	66.43	5.17	1.90×10^{-4}
Epi0id	1.14×10^{3}	81.78	3.27	1.61×10^{3}	76.40	0.050	7.17×10^{3}	61.52	3.20×10^{-3}	4.76×10^{3}	52.94	0.014	29.47	44.36	8.44×10^{-5}
$E\theta^2$	15.13	1.32	0.043	39.00	2.42	1.21×10^{-3}	8.62	0.12	3.85×10^{-6}	20.91	0.44	6.15×10^{-5}	0.50	1.69	1.43×10^{-6}
$E\theta^2$ **(sb)**	386.16	-	1.10	306.55	-	9.48×10^{-3}	165.59	-	7.40×10^{-5}	149.93	-	4.41×10^{-4}	6.24	-	1.79×10^{-5}
No ShwE	15.54	-	0.044	69.61	-	2.15×10^{-3}	68.48	-	3.06×10^{-5}	75.67	-	2.22×10^{-4}	9.49	-	2.72E-05